

On Landau's Eigenvalue Theorem for Line-of-Sight MIMO Channels

Andrea Pizzo *Member, IEEE*, Angel Lozano, *Fellow, IEEE*

Abstract—An alternative derivation is provided for the degrees of freedom (DOF) formula on line-of-sight (LOS) channels via Landau's eigenvalue theorem for bandlimited signals. Compared to other approaches, Landau's theorem provides a general framework to compute the DOF in arbitrary environments, this framework is herein specialized to LOS propagation. The development shows how the spatially bandlimited nature of the channel relates to its geometry under the paraxial approximation that applies to most LOS settings of interest.

Index Terms—Degrees of freedom, line-of-sight MIMO, paraxial approximation, Landau's eigenvalue theorem.

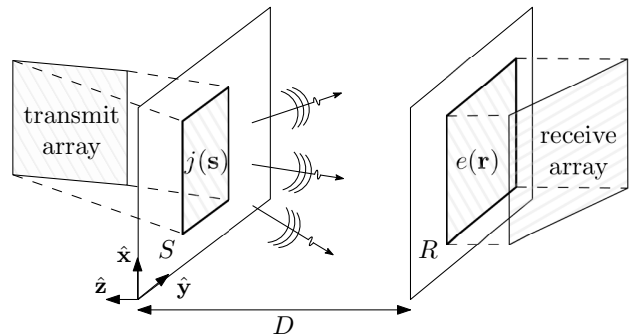


Fig. 1. LOS communications between continuous arrays.

I. INTRODUCTION

The number of distinct waveforms able to transport information via electromagnetic waves is an inherent property of a physical channel. It is upper bounded by the number of degrees of freedom (DOF), a quantity of interest in information theory [1]–[3], optics [4]–[8], electromagnetism [9]–[11], and signal processing [12], [13]. Given the continuous nature of channels, waveforms span an infinite-dimensional space, yet the noise allows for a certain error in the representation [10]. Channels are thus amenable to a discrete representation over a space of approximately DOF dimensions [14].

There are various ways to compute the number of DOF in a wireless channel, say by leveraging diffraction theory [4]–[6], by studying the eigenvalues of the Green's operator [3], [7]–[9], or by pursuing a signal-space approach [1], [13]. This paper provides an alternative derivation via Landau's eigenvalue theorem for multidimensional bandlimited signals (or fields) [15]. Analogously to time-domain waveforms of finite bandwidth, an electromagnetic channel may be regarded as spatially bandlimited due to a low-pass filtering behavior of the propagation [1], [9], [13]. In this analogy, time is replaced by space and frequency by spatial-frequency (or wavenumber) [14].

Originally devised for waveform channels [16], Landau's theorem has been generalized to electromagnetic

propagation [15], and lately applied to non-line-of-sight (NLOS) channels [13]. Prompted by the interest in LOS multiple-input multiple-output (MIMO) communication at high frequencies [17], here the connection is drawn with such channels under the paraxial approximation that holds when the propagation is focused about the axis connecting the two arrays [18]. The development builds on signal theory concepts, without relying on unconventional mathematics. A bridge between LOS and NLOS propagation is also uncovered, with implications for MIMO communication and Nyquist reconstruction at high frequencies.

Notation: \mathcal{F}_n is the n -dimensional Fourier operator, $(\mathcal{F}_n h)(\mathbf{f}) = \int_{\mathbb{R}^n} h(\mathbf{t}) e^{-j2\pi \mathbf{f}^T \mathbf{t}} d\mathbf{t} = g(\mathbf{f})$, whereas \mathcal{F}_n^{-1} is its inverse, $(\mathcal{F}_n^{-1} g)(\mathbf{t}) = h(\mathbf{t})$, with the shorthand notation $\mathcal{F}_1 = \mathcal{F}$ and $\mathcal{F}_1^{-1} = \mathcal{F}^{-1}$. In turn, $(\mathbb{1}_R h)(\mathbf{t}) = \mathbb{1}_R(\mathbf{t})h(\mathbf{t})$ with $\mathbb{1}_R(\mathbf{t})$ the indicator function of a set $R \subset \mathbb{R}^n$ while R_A is the set obtained by applying any invertible linear transform A to the axes of R , and $m(\cdot)$ is the Lebesgue measure.

II. PLANE-WAVE REPRESENTATION OF LOS CHANNELS

Consider two n -dimensional continuous-space arrays ($n = 1$ or 2) communicating with scalar electromagnetic waves at wavelength λ in a 3D free-space environment. We denote by D the distance between the array centroids. Capitalizing on that an arbitrary source can always be replicated by a flat source on a given plane thanks to Huygen's principle [19], we let $S \subset \mathbb{R}^n$ and $R \subset \mathbb{R}^n$ be

A. Pizzo and A. Lozano are with Univ. Pompeu Fabra (email: {andrea.pizzo, angel.lozano}@upf.edu). Work supported by the European Research Council under the H2020 Framework Programme/ERC grant agreement 694974, by the ICREA Academia program, by the European Union-NextGenerationEU, and by the Fractus-UPF Chair on Tech Transfer and 6G.

the projections—respecting the respective centroids—of the source and receive arrays onto parallel planes ($n = 2$) or parallel lines ($n = 1$). The normal to these planes or lines aligns with the z -axis, as shown in Fig. 1 for $n = 2$. The scalar electromagnetic field $e(\mathbf{r})$, $\mathbf{r} \in R$, is the image of a current density $j(\mathbf{s})$, $\mathbf{s} \in S$, through a linear channel operator \mathcal{G} as

$$e(\mathbf{r}) = (\mathcal{G}j)(\mathbf{r}) = \int_S h(\mathbf{r}, \mathbf{s}) j(\mathbf{s}) d\mathbf{s} \quad (1)$$

where $h(\mathbf{r}, \mathbf{s})$ is the space-variant kernel induced by the operator, as dictated by the physical environment. In LOS, it is found by solving [19]

$$\nabla^2 e(\mathbf{r}) + \left(\frac{2\pi}{\lambda}\right)^2 e(\mathbf{r}) = j \frac{2\pi\eta}{\lambda} j(\mathbf{r}) \quad (2)$$

with η the impedance. The kernel solving (2) is known to be given by $h(\mathbf{r}, \mathbf{s}) = -j \frac{2\pi\eta}{\lambda} G(\mathbf{r}, \mathbf{s})$ with [19, Sec. 1.3.4]

$$G(\mathbf{r}, \mathbf{s}) = \frac{e^{j2\pi \frac{r}{\lambda}}}{4\pi r} \quad (3)$$

the scalar Green's function, where $r = \|(\mathbf{r} - \mathbf{s}, -D)\|$ reveals the space-invariant nature of LOS channels [20]. The foregoing kernel can also be represented as the plane-wave decomposition [20, Eq. 12]

$$h(\mathbf{r}, \mathbf{s}) = \frac{\eta}{2\lambda} \int_{\mathbb{R}^n} \frac{e^{-j2\pi\kappa_z D}}{\kappa_z} e^{j2\pi\mathbf{k}^T(\mathbf{r}-\mathbf{s})} d\mathbf{k} \quad (4)$$

with

$$\kappa_z = \begin{cases} \sqrt{1/\lambda^2 - \|\mathbf{k}\|^2} & \|\mathbf{k}\| \leq 1/\lambda \\ j\sqrt{\|\mathbf{k}\|^2 - 1/\lambda^2} & \|\mathbf{k}\| > 1/\lambda \end{cases} \quad (5)$$

such that $\|\mathbf{k}\|^2 + \kappa_z^2 = 1/\lambda^2$ for every wave vector¹ \mathbf{k} . Properly normalized, the real parts of (\mathbf{k}, κ_z) are the cosines of the angles subtended by each plane wave with the axes, while $\lambda\|\mathbf{k}\| = \sin\theta$ and $\lambda\kappa_z = \cos\theta$ given $\theta \in [0, \pi/2]$ as the plane-wave's angle with the z -axis.

III. PARAXIAL APPROXIMATION IN THE WAVENUMBER DOMAIN

The *paraxial approximation* applies when, away from the source, propagation is focused about the axis connecting with the receiver (the z -axis in our case) [18]. It entails $D \gg L$ with L the maximum array dimension, such that the phase and magnitude of (3) satisfy [7], [17]

$$r \approx \begin{cases} D + \frac{\|\mathbf{r} - \mathbf{s}\|^2}{2D} & \text{(phase)} \\ D & \text{(magnitude)} \end{cases} \quad (6)$$

where the phase's behavior follows from $\sqrt{1+x} \approx 1 + \frac{x}{2}$ for small $x = \|\mathbf{r} - \mathbf{s}\|^2/D^2$.

¹For notational convenience, the wavenumber domain in [14, Ch. 8] is rescaled by $1/2\pi$, corresponding to the spatial frequency domain.

The paraxial approximation has its translation to the wavenumber domain. From $|\sin\theta| \ll 1$, it follows that $\|\mathbf{k}\| \ll 1/\lambda$; then, (5) satisfies [18]

$$\kappa_z \approx \begin{cases} 1/\lambda - \frac{\lambda\|\mathbf{k}\|^2}{2} & \text{(phase)} \\ 1/\lambda & \text{(magnitude)}. \end{cases} \quad (7)$$

It is shown in Appendix A that, under the paraxial approximation, (1) reduces to

$$e(\mathbf{r}) = (\widehat{\mathcal{G}}j)(\mathbf{r}) = \int_S e^{j2\pi\mathbf{s}^T \frac{\mathbf{r}}{\lambda D}} j(\mathbf{s}) d\mathbf{s} \quad (8)$$

for $\mathbf{r} \in R$. The uniform scaling transform $\mathbf{A} = \frac{1}{\lambda D} \mathbf{I}_n$ of the receiver's axes would yield, equivalently,

$$e(\mathbf{r}) = (\mathcal{H}j)(\mathbf{r}) = \int_S j(\mathbf{s}) e^{j\mathbf{s}^T \mathbf{r}} d\mathbf{s} \quad (9)$$

for $\mathbf{r} \in R_{\mathbf{A}}$. Hence, paraxial LOS channels amount to an n -dimensional inverse Fourier transform of the source density returning the received field [18]. The limitation of the source support that a transmit array imposes corresponds to a low-pass filtering operation, revealing the *spatially bandlimited* nature of electromagnetic fields [1], [9], [13]. With respect to the classical definition of a bandlimited signal in the frequency domain, here, the notion applies in the wavenumber domain [14, Ch. 8].

IV. KOLMOGOROV SPACE DIMENSIONALITY

Due to conservation of energy, $e(\mathbf{r})$ belongs to the Hilbert space V of square-integrable functions. This space is equipped with the norm $\|e\| = (\int_{\mathbb{R}^n} |e(\mathbf{r})|^2 d\mathbf{r})^{1/2}$ with $e(\mathbf{r})$ characterized by an infinite number of basis functions. The DOF provide a measure of the effective dimensionality of V , i.e., the minimum number N of basis functions needed to represent every element of V up to some accuracy. The degree of approximation of V by an N -dimensional subspace V_N is measured by the Kolmogorov N -width [14, Ch. 3.2]

$$d_N(V) = \inf_{\dim(V_N)=N} D_{V_N}(V) \quad (10)$$

with $D_{V_N}(V) = \sup_{e \in V} \inf_{e_N \in V_N} \|e - e_N\|$ the deviation between V and V_N according to a min-max criterion. The N -width in (10) is the smallest such deviation over all subspaces of dimension N . The DOF in V at any level of accuracy $0 < \sigma < 1$ is then

$$\text{DOF}_\sigma = \min\{N : d_N(V) \leq \sigma\} \quad (11)$$

whose existence is ensured by the spectral theorem for self-adjoint operators. Precisely, for any Hilbert-Schmidt operator \mathcal{H} , we have that [14, Eq. 3.56]

$$\text{DOF}_\sigma = \min\{N : \lambda_N \leq \sigma\} \quad (12)$$

where λ_N is the N th smallest eigenvalue of $\mathcal{H}\mathcal{H}^*$ (composition of \mathcal{H} with its adjoint \mathcal{H}^*). The discrete counterpart is the spectral theorem for Hermitian matrices, with λ_N the N th smallest eigenvalue of $\mathbf{H}\mathbf{H}^*$.

V. DOF

A. Bandlimited Waveforms

As the observation interval T increases, a waveform concentrates within a bandwidth B (in Hz), with the maximum simultaneous concentration in time and frequency dictated by the uncertainty principle [14, Ch. 2]. This behavior is specified by [16]

$$\mathcal{T}_T \mathcal{B}_B \mathcal{T}_T \phi_i(t) = \lambda_i \phi_i(t) \quad (13)$$

where $\mathcal{T}_T = \mathbb{1}_{|t| \leq T/2}$ and $\mathcal{B}_B = \mathcal{F}^{-1} \mathbb{1}_{|f| \leq B} \mathcal{F}$ correspond to time-limiting to $T/2$ and frequency-limiting to B [14, Ch. 3.4.1]. Rewriting (13) as $\mathcal{H}\mathcal{H}^*$ with

$$\mathcal{H} = \mathcal{T}_T \mathcal{F}^{-1} \mathbb{1}_{|f| \leq B} \quad \mathcal{H}^* = \mathbb{1}_{|f| \leq B} \mathcal{F} \mathcal{T}_T, \quad (14)$$

the spectral theorem yields an eigensolution. Specifically, for any σ , (12) is obtained by spectral concentration after letting T grow while keeping B fixed, giving [16, Eq. 2]

$$\text{DOF}_\sigma = \text{DOF} + \frac{1}{\pi^2} \log\left(\frac{1-\sigma}{\sigma}\right) \log T + o(\log T) \quad (15)$$

where

$$\text{DOF} = 2BT. \quad (16)$$

By symmetry, (15) can also be obtained from an operator $\mathcal{B}_B \mathcal{T}_T \mathcal{B}_B$, scaling the frequency axis by B and letting B grow while keeping T fixed.

B. Spatially Bandlimited Fields

Generalization to multidimensional signals (or fields) is achieved by replacing time with space, and frequency with wavenumber. The concentration of a spatially bandlimited field of wavenumber support $\mathbf{k} \in K \subset \mathbb{R}^n$ observed on a region $R_A \subset \mathbb{R}^n$ is ruled by [15, Eq. 10] [14, Ch. 3.5]

$$\mathcal{T}_{R_A} \mathcal{B}_K \mathcal{T}_{R_A} \phi_i(\mathbf{r}) = \lambda_i \phi_i(\mathbf{r}) \quad (17)$$

where $\mathcal{T}_{R_A} = \mathbb{1}_{R_A}$ and $\mathcal{B}_K = \mathcal{F}_n^{-1} \mathbb{1}_K \mathcal{F}_n$ correspond to space-limiting to R_A and wavenumber-limiting to K . Rewriting (17) as $\mathcal{H}\mathcal{H}^*$ with

$$\mathcal{H} = \mathcal{T}_{R_A} \mathcal{F}_n^{-1} \mathbb{1}_K \quad \mathcal{H}^* = \mathbb{1}_K \mathcal{F}_n \mathcal{T}_{R_A}, \quad (18)$$

an eigensolution of (17) is obtained as [15],

$$\text{DOF}_\sigma = \text{DOF} + \frac{1}{\pi^2} \log\left(\frac{1-\sigma}{\sigma}\right) \log \det(\mathbf{A}) + o(\log \det(\mathbf{A})) \quad (19)$$

where

$$\text{DOF} = m(K)m(R_A). \quad (20)$$

Spectral concentration arises as R_A varies over $\mathcal{A}R$ with fixed R and growing $\det(\mathbf{A})$, while K is fixed [14, Ch. 3.5.4]. By symmetry, (19) is also obtainable from an operator $\mathcal{B}_K \mathcal{T}_{R_A} \mathcal{B}_K$ after scaling the wavenumber domain by a growing $\det(\mathbf{A})$ while R and K are fixed.

From (20), we can recover (16) by setting $R = \{|t| \leq 1/2\}$ and $K = \{|f| \leq B\}$ while turning \mathbf{A} into T .

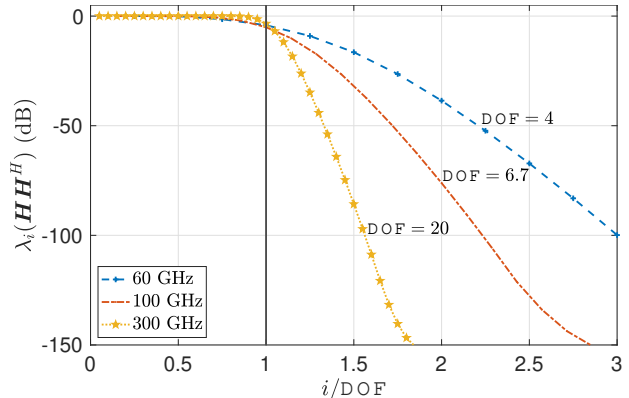


Fig. 2. Normalized sorted eigenvalues of $\mathbf{H}\mathbf{H}^* \in \mathbb{C}^{N \times N}$ at various frequencies for ULAs with $L = 0.2$ m and $D = 10L$. Smooth curves are obtained by having $N \gg \text{DOF}$.

C. Paraxial LOS Channels

Owing to the Fourier relationship between source current and receive field in (9), restricting the source to S is tantamount to limiting the wavenumber to $K = S$ at the receiver. In turn, the receiver region is R_A with $\mathbf{A} = \frac{1}{\lambda D} \mathbf{I}_n$. The DOF are then an instance of (20), precisely

$$\text{DOF} = m(S)m(R_A) = \frac{m(S)m(R)}{(\lambda D)^n} \quad (21)$$

given $m(R_A) = \det(\mathbf{A})m(R)$. Spectral concentration is achieved with R and S fixed while λD shrinks, whereby the receive array becomes magnified from the vantage of the source and the spatial resolution sharpens. Although such concentration could potentially be squeezed by the paraxial approximation, which requires D to be large, it is shown in Sec. VI-B that such squeeze is rather inconsequential.

Symmetry may be leveraged to alternatively obtain (21) via $\mathcal{B}_K \mathcal{T}_{R_A} \mathcal{B}_K$. This amounts to swapping source and receiver, with the same result due to reciprocity [20].

Let $\mathbf{H} \in \mathbb{C}^{N \times N}$ be the MIMO channel matrix obtained by sampling two 1D continuous arrays of size $L = 0.2$ m. The eigenvalues of $\mathbf{H}\mathbf{H}^*$ are plotted in Fig. 2, sorted and normalized by $\text{DOF} = L^2/(\lambda D)$. The frequency is $\{60, 100, 300\}$ GHz and $D = 10L$, complying with the paraxial approximation. Expectedly, the eigenvalues polarize into two levels as the carrier frequency increases due to spectral concentration.

VI. LOS AND NLOS PROPAGATION

A. DOF

NLOS channels are specified by $h(\mathbf{r}, \mathbf{s})$, space-variant because of multipath propagation introducing a separate dependence on the source and receiver locations [20].

For 1D arrays of dimensions L_s and L_r , under isotropic scattering [1, Eq. 27]

$$\text{DOF} = \min\left(\frac{L_s}{\lambda/2}, \frac{L_r}{\lambda/2}\right). \quad (22)$$

In complete generality, with n -dimensional arrays and wavenumber supports $K_s \subset \mathbb{R}^n$ and $K_r \subset \mathbb{R}^n$,

$$\text{DOF} = \min\left(m(K_r)m(C_{A_r}), m(K_s)m(C_{A_s})\right) \quad (23)$$

where the source and receiver have been expressed as linear transformations of a unit-measure set $C \subset \mathbb{R}^n$ with transform matrices A_s and A_r , i.e., $S = C_{A_s}$ and $R = C_{A_r}$. Spectral concentration occurs when $\min(\det(A_s), \det(A_r))$ grows while K_s and K_r are fixed.

To see how (23) specializes to (22), it suffices to let $C = \{|x| \leq 1/2\}$ and $K_s = K_r = \{|\kappa_x| \leq 1/\lambda\}$ while A_s and A_r become the scalars L_s and L_r .

From (23), we can also geometrically recover the result for paraxial LOS channels in (21). The solid angle subtended by the source at the receiver is $m(S)/D^n$. From the paraxial approximation, $\sin(\theta) \approx \theta$ while $\lambda\|\mathbf{k}\| = \sin\theta$, hence $m(K_r) = m(S)/(\lambda D)^n$. Due to reciprocity, $m(K_s) = m(R)/(\lambda D)^n$ from the vantage of the source. Plugging these results into (23) yields (21).

There are two terms in (23), modeling the separate scattering at both ends of the link and the ensuing space variance of NLOS channels [20]. In contrast, there is only a term in (21), as LOS propagation puts source and receiver in one-to-one correspondence, leading to space invariance.

Also noteworthy is that, while in LOS channels S and R are the projections of the source and receive arrays, in NLOS channels, these are the actual array apertures as the array orientations are embedded into the angular selectivity of the local scattering.

B. Asymptotic Regimes

Another difference between (21) and (23) is in their regimes of relevance, where eigenvalues polarize into two levels (see Fig. 2) and asymptotic results can be leveraged [17]. To bring out the key concept, consider rectangular arrays of dimensions $L_{s,i}$ and $L_{r,i}$, $i = 1, \dots, n$, which arise from the transformation of a unitary square C by

$$A_s = \text{diag}(\{L_{s,i}\}_{i=1}^n) \quad (24)$$

$$A_r = \text{diag}(\{L_{r,i}\}_{i=1}^n). \quad (25)$$

The spectra of NLOS channels concentrate for

$$\min\left(\prod_{i=1}^n \frac{L_{s,i}}{\lambda}, \prod_{i=1}^n \frac{L_{r,i}}{\lambda}\right) \gg 1, \quad (26)$$

implying electrically large arrays. Alternatively, paraxial LOS channels require

$$\sqrt[n]{\prod_{i=1}^n \frac{L_{s,i}}{\lambda} \prod_{i=1}^n \frac{L_{r,i}}{\lambda}} \gg \frac{D}{\lambda} \gg \max_{i=1, \dots, n} \left(\frac{L_{s,i}}{\lambda}, \frac{L_{r,i}}{\lambda}\right) \quad (27)$$

where the first inequality ensures spectral concentration in (21) and the second one embodies the paraxial approximation. (As a by-product of the first inequality, D is also incompatible with planar wavefronts.)

Welcomely, (27) delimits a broad range of validity for the developed theory. With squared arrays of size L , setting $D = 10L$ as a reasonable concretization of the second inequality, the first one yields $D/\lambda \gg 100$; at 100 GHz, this amounts to $D \gg 0.3$ m. Rescaling one axis by $\beta \geq 1$ and the other one by $1/\beta$, to keep the array apertures fixed while altering their aspect ratio, setting $D = 10\beta L$ yields $D/\lambda \gg 100\beta^2$; at 100 GHz with $\beta = 4$, this gives $D \gg 4.8$ m.

C. Nyquist Sampling

The DOF per spatial unit correspond to the sampling density μ (in samples/m^{*n*}) needed for reconstruction [13], extending the classical notion of Nyquist rate (samples/s) to n -dimensional fields.

Recalling (23) for NLOS channels, at the receiver

$$\mu_r = \frac{\text{DOF}}{m(R)} = m(K_r). \quad (28)$$

This is highest under isotropic scattering, when K_r is an n -dimensional disk of unit radius [13], [20] leading to $\lambda/2$ -sampling and to hexagonal sampling with density π/λ^2 , respectively when $n = 1$ and $n = 2$ [13]. Scattering selectivity shrinks $m(K_r)$, rendering the sampling sparser.

In turn, recalling (21) for LOS channels, at the receiver

$$\mu_r = \frac{\text{DOF}}{m(R)} = \frac{m(S)}{(\lambda D)^n} \quad (29)$$

which depends on sheer geometry (source dimension, wavelength, and range), rather than on the scattering selectivity. An inspection of (29) also reveals that LOS channels can be reconstructed more efficiently due to a lower DOF density. For instance, $\lambda/2$ -sampling with $n = 1$ implies $D = L_s/2$, which is unfeasible under the paraxial approximation.

D. Rayleigh Spacing for LOS Channels

Consider 1D arrays and let N_s and N_r be the transmit and receive antenna numbers, with uniform spacings $\delta_s = 1/\mu_s$ and $\delta_r = 1/\mu_r$ (in m/sample); these are reciprocals of the Nyquist densities. For LOS channels, from (29) and $L_s = (N_s - 1)\delta_s$, we obtain $\delta_s\delta_r = \frac{\lambda D}{N_s - 1}$. From reciprocity, we further infer $\delta_s\delta_r = \frac{\lambda D}{N_r - 1}$. To prevent aliasing in the wavenumber domain, the antenna spacings must yield the largest spectrum separation, namely

$$\delta_s\delta_r = \frac{\lambda D}{N_{\max} - 1} \quad (30)$$

with $N_{\max} = \max(N_r, N_s)$.

The so-called Rayleigh spacings d_s and d_r , which enable full DOF exploitation and are therefore optimum at a high signal-to-noise ratio, satisfy [17, Eq. 10]

$$d_s d_r = \frac{\lambda D}{N_{\max}}, \quad (31)$$

which coincides with (30) when $N_{\max} \gg 1$, i.e., when Nyquist sampling attains perfect reconstruction [13].

VII. CONCLUSION

The paraxial approximation endows LOS channels with a bandlimited nature in the wavenumber domain, a nature from which the DOF formula can be obtained via Landau's eigenvalue theorem [15], [16]. As in NLOS channels [1], [2], the ensuing DOF are determined by the size and geometry of the arrays and the angular selectivity of the environment. LOS channels are inherently geometrical [17], with the angular selectivity dictated by the solid angle subtended by the source at the receiver. Three physical effects play a role: *zooming*, inversely proportional to the wavelength, *skewing*, function of the relative array orientations, and *magnification* as the communication range shrinks.

APPENDIX A

Plugging (7) into the plane-wave representation in (4),

$$\hat{h}(\mathbf{r}, \mathbf{s}) = \frac{\eta}{2\lambda} e^{-j2\pi \frac{D}{\lambda}} \int_{\mathbb{R}^n} e^{j\pi\lambda D \|\mathbf{k}\|^2} e^{j2\pi \mathbf{k}^T (\mathbf{r}-\mathbf{s})} d\mathbf{k}, \quad (32)$$

from which, removing unwanted constants,

$$\hat{h}(\mathbf{x}) = \int_{\mathbb{R}^n} e^{j\pi\lambda D \|\mathbf{k}\|^2} e^{j2\pi \mathbf{k}^T \mathbf{x}} d\mathbf{k} \quad (33)$$

where $\mathbf{x} = \mathbf{r} - \mathbf{s}$. Eq. (33) can be computed independently along each axis, e.g., along the x -axis,

$$\hat{h}(x) = \int_{-\infty}^{\infty} e^{j\pi\lambda D \kappa_x^2} e^{j2\pi \kappa_x x} d\kappa_x. \quad (34)$$

We recall that [21, Eq. 7.4.6],

$$\int_{-\infty}^{\infty} e^{-\frac{\pi}{a} f^2} e^{j2\pi f t} df = \sqrt{\frac{a}{\pi}} e^{-at^2} \quad (35)$$

for any $a \in \mathbb{C}$ with $\text{Re}(a) > 0$. Contrasting (35) with (34), we set $a = \frac{j\pi}{\lambda D}$ to obtain $\hat{h}(x) = e^{-\frac{j\pi}{\lambda D} x^2}$ where all known constants have been omitted. The condition $\text{Re}(a) > 0$ maps to a lossy medium. Reintroducing vector notation to account for n -dimensional arrays and omitting all known constants,

$$\hat{h}(\mathbf{r}, \mathbf{s}) = e^{-\frac{j\pi}{\lambda D} \|\mathbf{r}-\mathbf{s}\|^2}. \quad (36)$$

Expanding and rearranging the quadratic terms in (36), we obtain [17]

$$\hat{h}(\mathbf{r}, \mathbf{s}) = \phi(\mathbf{r}) e^{j\frac{2\pi}{\lambda D} \mathbf{s}^T \mathbf{r}} \phi(\mathbf{s}) \quad (37)$$

where $\phi(\mathbf{x}) = \exp(-j\frac{\pi}{\lambda D} \|\mathbf{x}\|^2)$. The channel kernel entails two separable quadratic phase shifts and a cross

phase shift that depends on the relative source and receive locations. With the geometry known at each end of the link, $\phi(\mathbf{s})$ and $\phi(\mathbf{r})$ can be compensated for, yielding (8).

ACKNOWLEDGMENT

Comments and suggestions by Heedong Do, from POSTECH, are gratefully acknowledged.

REFERENCES

- [1] A. S. Y. Poon, R. W. Brodersen, and D. N. C. Tse, "Degrees of freedom in multiple-antenna channels: a signal space approach," *IEEE Trans. Inf. Theory*, vol. 51, no. 2, pp. 523–536, Feb 2005.
- [2] A. Ozgur, O. Lévêque, and D. Tse, "Spatial degrees of freedom of large distributed MIMO systems and wireless ad hoc networks," *IEEE J. Sel. Areas Commun.*, vol. 31, no. 2, pp. 202–214, 2013.
- [3] M. Desgroseilliers, O. Lévêque, and E. Preissmann, "Spatial degrees of freedom of MIMO systems in line-of-sight environment," in *IEEE Int. Symp. Inf. Theory*, 2013, pp. 834–838.
- [4] G. Toraldo di Francia, "Resolving power and information," *J. Opt. Soc. Am.*, vol. 45, no. 7, pp. 497–501, Jul 1955.
- [5] A. Walther, "Gabor's theorem and energy transfer through lenses," *J. Opt. Soc. Am.*, vol. 57, no. 5, pp. 639–644, May 1967.
- [6] A. Thaning, P. Martinsson, M. Karelin, and A. T. Friberg, "Limits of diffractive optics by communication modes," *J. Opt.*, vol. 5, no. 3, pp. 153–158, mar 2003.
- [7] D. A. B. Miller, "Communicating with waves between volumes: evaluating orthogonal spatial channels and limits on coupling strengths," *Appl. Opt.*, vol. 39, no. 11, pp. 1681–1699, Apr 2000.
- [8] R. Piestun and D. A. B. Miller, "Electromagnetic degrees of freedom of an optical system," *J. Opt. Soc. Am. A*, vol. 17, no. 5, pp. 892–902, May 2000.
- [9] O. M. Bucci and G. Franceschetti, "On the degrees of freedom of scattered fields," *IEEE Trans. Antennas Propag.*, vol. 37, no. 7, pp. 918–926, 1989.
- [10] M. D. Migliore, "On the role of the number of degrees of freedom of the field in MIMO channels," *IEEE Trans. Antennas Propag.*, vol. 54, no. 2, pp. 620–628, 2006.
- [11] J. Xu and R. Janaswamy, "Electromagnetic degrees of freedom in 2-D scattering environments," *IEEE Trans. Antennas Propag.*, vol. 54, no. 12, pp. 3882–3894, 2006.
- [12] R. A. Kennedy, P. Sadeghi, T. D. Abhayapala, and H. M. Jones, "Intrinsic limits of dimensionality and richness in random multipath fields," *IEEE Trans. Signal Process.*, vol. 55, no. 6, pp. 2542–2556, 2007.
- [13] A. Pizzo, A. D.-J. Torres, L. Sanguinetti, and T. L. Marzetta, "Nyquist sampling and degrees of freedom of electromagnetic fields," *IEEE Trans. Signal Process.*, 2022.
- [14] M. Franceschetti, *Wave Theory of Information*, Cambridge University Press, 2017.
- [15] M. Franceschetti, "On Landau's eigenvalue theorem and information cut-sets," *IEEE Trans. Inf. Theory*, vol. 61, no. 9, 2015.
- [16] H. J. Landau and H. Widom, "Eigenvalue distribution of time and frequency limiting," *J. Math. Anal. Appl.*, vol. 77, no. 2, pp. 469–481, 1980.
- [17] H. Do, N. Lee, and A. Lozano, "Reconfigurable ULAs for line-of-sight MIMO transmission," *IEEE Trans. Wireless Commun.*, vol. 20, no. 5, pp. 2933–2947, 2021.
- [18] J. W. Goodman, *Introduction to Fourier Optics*, McGraw-Hill, San Francisco, 1968.
- [19] W. C. Chew, *Waves and Fields in Inhomogenous Media*, Wiley-IEEE Press, 1995.
- [20] A. Pizzo, L. Sanguinetti, and T. L. Marzetta, "Spatial characterization of electromagnetic random channels," *IEEE Open J. Commun. Soc.*, vol. 3, pp. 847–866, 2022.
- [21] M. Abramowitz and I. A. Stegun, *Handbook of mathematical functions*, Dover Publications, New York, 1972.